DYNAMIC VARIATION MODEL OF DELAY PROFILES IN LINE-OF-SIGHT (LOS) INDOOR ENVIRONMENTS FOR BROADBAND TRANSMISSION

Naoki KITA[†,†††], Wataru YAMADA[†], Daisuke MORI[††], and Makoto ANDO[†††]
[†]NTT Access Network Service Systems Laboratories, Nippon Telegraph and Telephone Corporation
[††]Wireless Communication Division, NTT Advanced Technology Corporation
[†††]Tokyo Institute of Technology
[†, ††] 1-1 Hikari-no-oka, Yokosuka-shi, Kanagawa, 239-0847, Japan
[†††]2-12-1 Ookayama, Meguro-ku, Tokyo, 152-8552, Japan
E-mail: [†]{nkita, wataru-y}@ansl.ntt.co.jp, [††]{mori}@yrp.ntt-at.co.jp,
[†††]mando@antenna.ee.titech.ac.jp

1. Introduction

Wireless Local Area Network (WLAN) systems including HIPERLAN/2, IEEE802.11a, and HiSWANa [1] have been developed and provide transmission rates of up to 54 Mbps for short range communication in indoor environments. The maximum transmission speed of these WLAN systems can be achieved in locations where the received level becomes high such as in a line-of-sight (LOS) region. Therefore, especially in an office environment, establishing multiple base stations (BSs) in one room is commonplace in order to increase the LOS regions where users can communicate at the maximum transmission speeds. Therefore, these LOS regions represent an important area as a major radio propagation environment for indoor wireless communications using WLAN systems. Furthermore, future WLAN systems, which will provide transmission speeds of over 100 Mbps, are developing and are attracting much attention [e. g. 2]. The Multiple-Input Multiple-Output (MIMO) technique is considered a candidate to achieve such high transmission speeds. According to the development of such a high-speed wireless access system, various studies on indoor multipath propagation characteristics have been conducted [e.g. 3], but there is still a lack of detailed studies on the broadband (MIMO) channel model for indoor LOS environments.

This paper proposes a new dynamic delay profile model in LOS indoor environments for designing the broadband WLAN systems based on measured results in terms of the variation characteristics of the front wave component. Furthermore, the difference between using conventional and the proposed delay profile model in evaluating the MIMO channel capacity is also presented.

2. Conventional broadband WLAN channel model

The Medbo model [4] is representative of a channel model for broadband Single-Input Single-Output (SISO) WLAN systems. The delay profile (delay tap) models such as that shown in Fig. 1 for five different indoor scenarios are prepared for designing SISO WLAN systems [4]. Recently, the broadband MIMO WLAN channel model, which is an extension of the Medbo model, has also been prepared for the design of broadband MIMO WLAN systems in IEEE 802.11 TGn (Task Group n) [5]. The MIMO channel matrix, H_T, for each tap, at one instance of time, in the delay profile model for some different indoor environments comprises a fixed (constant, LOS) matrix and a Rayleigh (variable, NLOS) matrix expressed as Eq. (1).

$$H_T = \sqrt{P_T}\left(\sqrt{\frac{K_r}{K_r+1}}H_F + \sqrt{\frac{1}{K_r+1}}H_v\right) \tag{1}$$

where P_T is the power of each tap, K_r is the Nakagami-Rician K-factor, H_F is the fixed LOS matrix, and H_v is the variable NLOS matrix. The LOS K-factor is applicable only to the first tap while the K-factor of all the other taps remains at -∞ dB. Such a scheme for LOS channel modeling was adopted for not only a MIMO WLAN channel, but also the conventional SISO WLAN channel. That is, the level variation of the first tap is assumed to conform to the Nakagami-Rician distribution, and the level variation of all the other taps is assumed to conform to the Rayleigh distribution for SISO or MIMO. However, there is still a lack of detailed study on the value of K_r, or the distribution itself of the level variation for the first tap in an indoor LOS environment.

3. Variation characteristics of first tap and delay taps in real indoor LOS environments

Measurements of the delay profile snapshots were carried out in three representative indoor

ISBN: 89-86522-79-9 94460©KEES

LOS environments to reveal the characteristics of level variation for the first tap and the other taps. The measurement conditions and features are given in Tables I and II, respectively. The measurements were performed along some measurement routes in each room. A transmitter on a trolley was used as the mobile station (MS) and traveled along these routes at a constant speed of approximately 0.5 m/sec. A delay profile snapshot was acquired every 102.3 msec. The measuring trolley put out electric pulse about running distance were recorded simultaneously. The measured delay profile snapshots, which correspond to 5 cm segments, were analyzed off-line.

Figure 2 shows an example of the acquired delay profile snapshots (portion), and Fig. 3 shows an example of the level variation in the front wave (corresponding to the level variation of the first tap) for a relative moving distance. The data of the front waves were extracted from the delay profile snapshots such as that shown in Fig. 2 while satisfying the Wide Sense Stationary (WSS) condition. The data shown in Figs. 2 and 3 were acquired in the conference room (corresponding to the bottom of Table I). The data such as that shown in Figs. 2 and 3 in all environments given in Table I were acquired and analyzed in terms of the cumulative probability distribution. Furthermore, the data from the delay waves in the acquired delay profile snapshots and those for the front waves were treaded in the same way.

Examples of the acquired cumulative probability distribution of the relative level of the front wave and delay waves are shown with the calculated distribution in Figs. 4(a) and 4(b), respectively. The solid line in Figs. 4(a) and 4(b) represent the measured distribution of the relative level of the front wave and delay waves, respectively, and the dotted lines in the figures represent the calculated Nakagami-Rician distribution (K-factor = 3 and 6 dB) and Rayleigh distribution, respectively. In Fig. 4(a), the measured distribution of the relative level of the front wave does not agree with the calculated Nakagami-Rician distribution that is assumed for the level variation of the first tap in the conventional delay profile models. In Fig. 4(b), the measured distributions of the relative level of the delay waves (only at 50, 100, 150, and 200 nsec are shown in Fig. 4(b) as examples) are in good agreement with the calculated Rayleigh distribution that is assumed for the level variation of all the delay taps except for the first tap in the conventional delay profile models. These results are for the case in the conference room, but similar trends were observed for all other cases in Table I.

In the next section, we describe a new model for the level variation of the first tap that agrees with the measured characteristics of the level variation of the front wave in a real indoor environment.

4. New level variation model for the first tap in real indoor LOS environments

The arrival waves that influence the level variation of the first tap in LOS environments are the direct and delayed waves that arrive at the first tap. For example, in the delay profile model shown in Fig. 1, where the interval between the first tap and second tap is 10 nsec, the arriving delayed waves within the first tap should be considered to be delayed waves where the difference in the path length compared to that of the direct wave is less than 1.5 m. The applicable delayed waves under this condition in general indoor LOS environments are reflected waves from the ceiling and floor. Therefore, a new level variation model of the first tap is proposed as a level variation due to those three waves (direct wave, reflected wave from ceiling, and reflected wave from floor) as shown in Fig. 5. The probability density function (p.d.f) of the three-wave distribution, $P(r)$, is given as follows [6]:

$$P(r)=\begin{cases}\dfrac{r^{1/2}}{\pi^2\sqrt{A_0A_1A_2}}K\left[\dfrac{\Delta^2}{A_0A_1A_2r}\right] & \left(\Delta^2 < A_0A_1A_2r\right)\\ \dfrac{r}{\pi^2\Delta}K\left[\dfrac{A_0A_1A_2r}{\Delta^2}\right] & \left(\Delta^2 \geq A_0A_1A_2r\right)\end{cases} \tag{2}$$

$$\Delta^2 = 1/16\cdot\{(r+A_0)^2-(A_1-A_2)^2\}\times\{(A_1+A_2)^2-(r-A_0)^2\}$$

where $K[x]$ is the complete 1st kind Elliptical Integral. The power ratio of the direct wave to the other two reflected waves is defined as Eq. (3).

$$K_3 \equiv \frac{A_0^{\,2}}{A_1^{\,2}+A_2^{\,2}} \tag{3}$$

The calculated examples of the cumulative probability of the three-wave distribution are shown to the left in Fig. 6. The Nakagami-Rician distribution examples are shown to the right in Fig. 6 as a reference. Figure 7 shows the cumulative probability distribution of the measured level of the front wave with the calculated cumulative probability of the three-wave distribution for each indoor scenario as given in Table I. The measured results in the conference room, office, and apartment are in very good agreement with the calculated three-wave distribution with K_3 = 8, 9, and 10 dB, respectively. It can be said that the three-wave distribution model for level variation of the first tap can represent the characteristics of the measured level variation of the front wave in real LOS indoor environments.

5. Difference between using conventional and proposed delay profile model in evaluating MIMO channel capacity

The channel capacity for broadband MIMO transmission in a LOS indoor environment was calculated using both the conventional model for a LOS large office [5] applying the Nakagami-Rician distribution with K_r = 6 dB to the first tap and the proposed model applying the three-wave distribution with K_3 = 6 dB to the first tap. A MIMO-OFDM (Orthogonal Frequency Division Multiplexing) system with the bandwidth of 20 MHz and the number of sub-carriers of 64 was assumed as the target system. We assumed 2 x 2, 4 x 4, and 8 x 8 (transmit x receive) antenna arrays. The separation between the antenna branches was assumed to be 1 λ. The channel capacity in terms of sub-carriers was calculated using the following equation.

$$C = \frac{\Delta f}{N}\sum_{n=1}^{N}\log_2 \det\left[I + (s/n_t)H(f+n\cdot\Delta f)H^{\diamond}(f+n\cdot\Delta f)\right] \quad \text{(bps/sub-carrier)} \quad (4)$$

where N is the number of sub-carriers, f is the frequency, Δf is the sub-carrier interval, s is the S/N which is 10 dB in this case. n_t is the number of branches for the transmit arrays, $H(f)$ is the broadband MIMO channel matrix, and $H^{\diamond}$ is the conjugate transpose of H. Figure 8 shows an example of the calculated results. The calculated value when using the proposed model is larger than that when using the conventional model. The difference in the calculation value between using the conventional and proposed model tends to be large when the number of antenna arrays is small. The difference at 50% of the cumulative probability is 88, 51, and 11 kbps/sub-carrier when assuming the use of 2x2, 4x4, and 8x8 antenna arrays, respectively.

6. Conclusions

A new dynamic variation model of the delay profiles in LOS indoor environments to design a broadband transmission system was proposed based on the measured delay profile snapshots in real indoor LOS environments. In particular, we conducted a detailed study on the variation characteristics of the front wave and revealed that the distribution of the level variation of the front wave conforms to a three-wave distribution. The results of this study were applied to the delay tap channel model. Furthermore, we presented the difference between using the conventional and newly proposed dynamic delay profile model based on the evaluation of the MIMO channel capacity.

Acknowledgement

The authors thank Mr. Atsuya Ando of the NTT Access Network Service Systems Laboratories, NTT Corporation, and Mr. Tetsuya Takao and Mr. Hironobu Watanabe of NTT Advanced Technology Corporation for their cooperation and encouragement throughout this study.

References

[1] A. Doufexi, et al., "A comparison of the HIPERLAN/2 and IEEE802.11a wireless LAN standards," *IEEE Commun. Mag*., vol. 40, pp. 172-180, May 2002.

[2] T. Sugiyama, et al., "Development of a novel SDM-COFDM prototype for broadband wireless access systems," in *Proc. of IEEE WCNC 2003*, vol. 1, pp. 55-60, March 2003.

[3] C. C. Chong, et al., "A new statistical wideband spatio-temporal channel model for 5-GHz band WLAN systems," *IEEE J. Select. Areas Commun*., vol. 21, pp. 139-150, Feb. 2003.

[4] J. Medbo, et al., "Channel models for HIPERLAN/2," ETSI/BLAN document no. 3ERI085B.

[5] V. Erceg, et al., "Indoor MIMO WLAN channel models," IEEE802.11 Wireless LANs, doc.: IEEE 802.11-03/161r2, Sept. 2003.

[6] J. W. Nicholson, "Generalization of a theorem due to sonine," *Quarterly J. Pure Appl. Math.*, vol. 48, pp. 321-329, 1920.

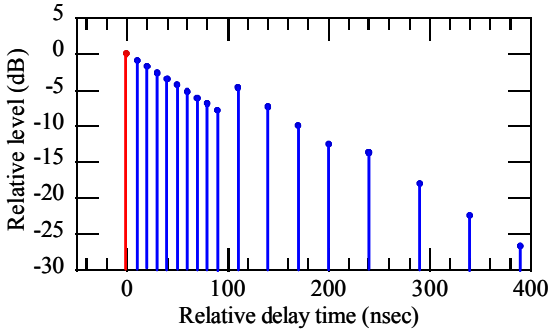

Figure 1. Example of delay tap model (Office)

Table I. Measurement Conditions (Left)
Table II. Measurement Features (Right)

Environment (size, (m))	Tx / Rx ant. height (m)
Apartment (3 * 8 * 3)	1.3 / 1.3
Office (20 * 30 * 3)	1.0 / 2.7
Conference room (7 * 13 * 3)	1.0 / 2.7

Detection method	Sliding correlation
Center freq.	5.2 GHz
PN code	1023 bits
Chip rate	60 MHz
Tx/Rx antenna	Dipole (2 dBi)
Polarization	Vertical

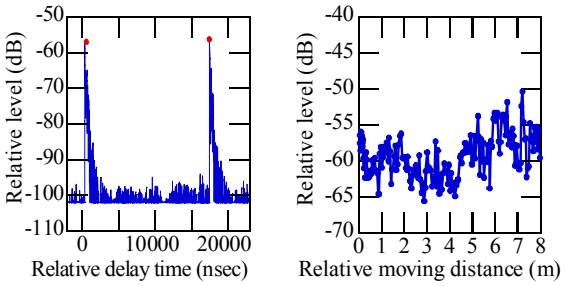

Figure 2. Example of acquired snapshots of delay profile in conference room (Left)
Figure 3. Example of level variation of front wave in conference room (Right)

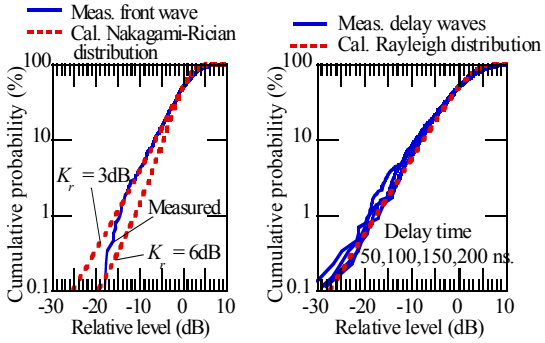

Figure 4(a). Example of variation characteristics of 1st delay wave (Left)
Figure 4(b). Example of variation characteristics of delay waves (Right)

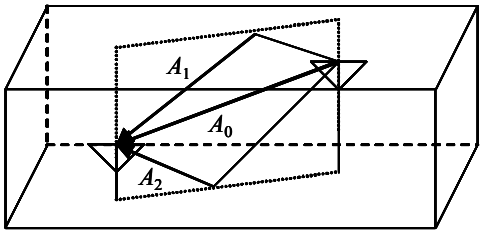

A_0, A_1, and A_2 : Direct, reflected by ceiling, and floor

Figure 5. Propagation model for variation of 1st tap

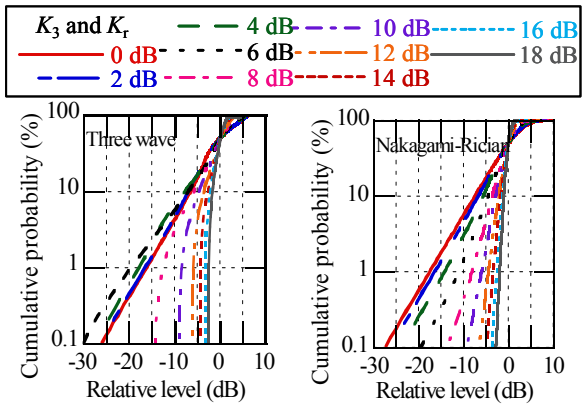

Figure 6. Example of cumulative probability of three wave distribution (Left) and Nakagami-Rician distribution (Right)

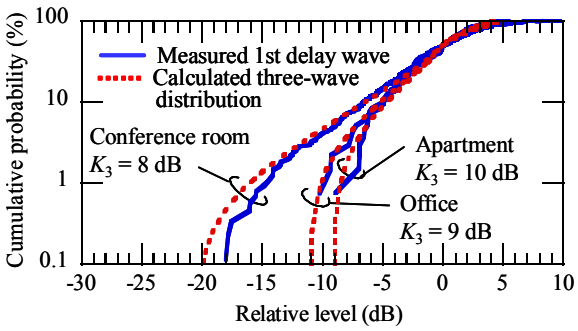

Figure 7. Variation characteristics of front wave

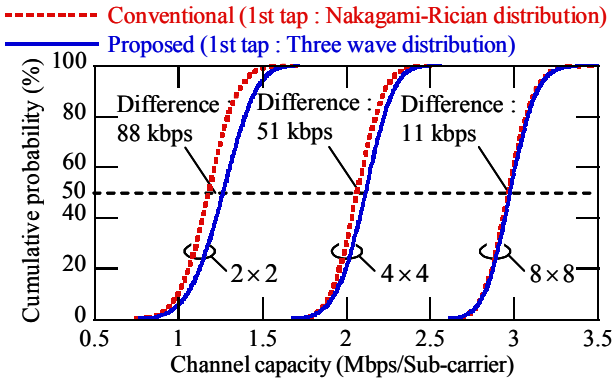

Figure 8. Calculation examples of channel capacity